Efficient Iterative Solution for Large Elasto-Dynamic Inverse Problems*

Fergyanto Efendy GUNAWAN** and Hiroomi HOMMA***

Convergence of the solver and the regularization are two important issues concerning an ill-posed inverse problem. The intrinsic regularization of the conjugate gradient method along iteration makes the method superior for solving an ill-posed problem. The solutions along iteration converge fast to an optimal solution. If the termination criterion is not satisfied, the solution will diverge to a solution which dominated by the noise. Reformulation of an ill-posed problem as an eigenvalue formulation gives a very convenient formula since it is possible to estimate an optimal regularization parameter and an optimal solution at once. For very large problems, the fast Fourier transformation could be implemented in the circulant matrix-vector multiplication. The developed method is applied to some inverse problems of elasto-dynamic and the accurate estimation was achieved.

Key Words: Inverse Analysis, Iterative Solution, CG-TLS Method, Tikhonov Regularization

1. Introduction

This paper is dealing with an ill-posed inverse problem. It is widely known that solving an ill-posed inverse problem is difficult. In the case of a well-posed problem, the attention only given to the solution method of the governing equation. An ill-posed inverse problem needs an additional treatment in term of the regularization to stabilize the numerical computation. Similar with the conventional problem, when the size of the problem becomes so large, an iterative solution method is preferable. A large size of data sometimes unavoidable. For example, data collected from an experiment of high speed impact of a small particle with a flexible plate, the sampling frequency should be very high to capture the event of high frequency oscillation. For that reason understanding the numerical behavior of an iterative solution in solving an inverse of elasto-dynamic problem is necessary.

Recently many researchers deal with application of the inverse analysis to some engineering problems. Two major fields in engineering, i.e., heat transfer[1),(2)] and image restoration[3)] receive much bigger attention than others. There are only a few publications concerning with inverse of elasto-dynamic problems[4),(5)], and no publication concerning a large elasto-dynamic inverse problem.

In his publication, Inoue[4)] employed a statistical method to minimize the noise in data. The numerical inversion is solved safely via the Tikhonov regularization and the singular value decomposition (SVD). Doyle[5)] minimizing the noise by using a digital filter and the inversion was done in the frequency domain. The frequency domain approach gives a possibility to solve a large inverse problem because the computational can be done efficiently. Even though the frequency domain method could handle a large size inverse problem, it is rather vague what criterion should be employed in designing the digital filter. There is a possibility that the digital filter also remove the significant spectrum on the data. The Tikhonov and SVD based method have been applied to various inverse problems and the method works well. The disadvantage of this method is that the decomposition is costly and only well suited when the data size is not large. At this circumstance, an iterative solution method offers an effective solution.

The termination criterion comes to play when an iterative solution method is being used. Basically, a conventional termination criteria such as minimize the objec-

* Received 29th November, 2002 (No. 02-4228)

** Department of Mechanical Engineering, Toyohashi University of Technology, 1–1 Hibarigaoka, Tempaku, Toyohashi, Aichi 441–8580, Japan.
E-mail: gunawan@mech.tut.ac.jp

*** International Cooperation Center for Engineering Education Development, Toyohashi University of Technology, 1–1 Hibarigaoka, Tempaku, Toyohashi, Aichi 441–8580, Japan. E-mail: homma@icceed.tut.ac.jp

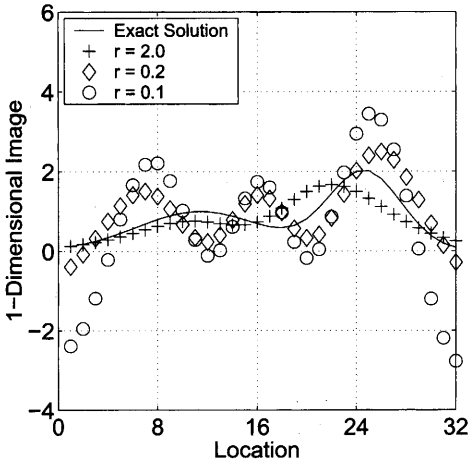

Fig. 1 An example of the failure of a least-square approach to an ill-posed problem

tive function, may lead unacceptable solution depending on the degree of the ill-posedness. It is easily shown that minimizing only an objective function without any numerical stabilization probably provides a wrong answer. As an example, a problem of one-dimensional image reconstruction can be taken. The optimal solution is computed by minimizing a residual vector $\boldsymbol{r}$ by means of the conjugate gradient (CG) iterative method and then various convergence limits of residual vector are evaluated. It is shown in Fig. 1 that for the lower residual vector, the discrepancy of the estimation and the exact solution becomes larger.

Tikhonov provides a method that an ill-posed inverse analysis should be solved by combining the minimum noise effect on the solution and the residual.

There are many iterative solution methods. Without an additional regularization only CG method suitable for solving an ill-posed inverse problem. The CG method which having an inherent regularization is a favorable iterative solution method. On iteration to search the optimal solution, the CG algorithm regularizes the solution vector. If careful treatment is not done for the convergence criterion, the obtained solution may be under-regularized or over-regularized.

As a summary, this paper focuses on an iterative solution method of CG algorithm for solving the ill-posed elasto dynamic problem. The results are given in the following order:

- A numerical study on convergence properties of the CG method is given in the next section.
- Accordingly, a combination of the CG method with the total least-square formulation (TLS) for determining the regularization parameter is presented.
- The method is evaluated by using a numerical simulation of some elasto dynamic inverse problems, i.e.,

— A single degree of freedom system (SDOF)
— Force estimation on a lateral impact of a flexible plate
— Identification of viscoelastic properties of GFRP

2. Convergence of Conjugate Gradient Method and Total Least-Square Formulation

The problem discussed in this paper is limited to a linear inverse problem, which can be written as a system of linear equation

$$\boldsymbol{A}\boldsymbol{x}=\boldsymbol{b} \tag{1}$$

where $\boldsymbol{A}$ is a $n\times n$ system matrix, $\boldsymbol{x}$ is an unknown, and $\boldsymbol{b}$ is a known right-hand side vector. The solution of $\boldsymbol{x}$ becomes ill-posed if the matrix $\boldsymbol{A}$ is not invertible. The invertibility of a system matrix can be quantified by their condition number. For a convolution problem, the system matrix $\boldsymbol{A}$ is a circulant matrix of the impulse response function. In engineering application, the impulse response function can be estimated by means of a numerical simulation, an analytical solution, or an experiment. Usually, the right-hand side vector $\boldsymbol{b}$ is an experimental result in which the interference of noise to the data is unavoidable. The larger condition number of the system matrix means the larger noise effect in the solution vector $\boldsymbol{x}$. Mostly, the solution of an ill-posed problem without numerical stabilization is not acceptable.

Tikhonov[6] re-defined the system of algebra equation Eq. (1) by introducing a stabilization parameter α as,

$$\min\{\|\boldsymbol{A}\boldsymbol{x}-\boldsymbol{b}\|_2+\alpha^2\|\boldsymbol{x}\|_2\} \tag{2}$$

or as normal equation

$$(\boldsymbol{A}^T\boldsymbol{A}+\alpha^2\boldsymbol{I})\boldsymbol{x}=\boldsymbol{A}^T\boldsymbol{b}. \tag{3}$$

For a small-scale problem, the above equation can be solved via the SVD method. The solution in term of the SVD is written as,

$$\boldsymbol{x}=\sum_{i=1}^{n}\frac{\sigma^2}{\sigma^2+\alpha^2}\frac{\boldsymbol{u}_i^T\boldsymbol{b}}{\sigma_i}\boldsymbol{v}_i \tag{4}$$

$$\boldsymbol{A}=\sum_{i=1}^{n}\boldsymbol{u}_i\sigma_i\boldsymbol{v}_i^T \tag{5}$$

If the SVD of the matrix $\boldsymbol{A}$ is available, then the L-curve technique can be used to compute the regularization parameter α. The value of α will lie somewhere between the highest and lowest singular values. To construct an L-curve, Eq. (4) must be solved for several values of α and then the norm of residual vector $\boldsymbol{A}\boldsymbol{x}-\boldsymbol{b}$ and the norm of vector $\boldsymbol{x}$ are plotted on an $x-y$ diagram in a log – log scale. The optimal regularization is the corner of the L-curve as depicted in Fig. 2.

In case of a large-scale inverse problem, the SVD is hardly computed, so then the iterative solution method like the CG method is preferable.

The CG algorithm for solving Eq. (3) can be seen in many publications. Hansen[6] proposed an implicit algorithm that can be applied without direct multiplication $\boldsymbol{A}^T\boldsymbol{A}$, which leads to unnecessary inaccuracy. In next section, we only explore the convergence properties of the CG algorithm.

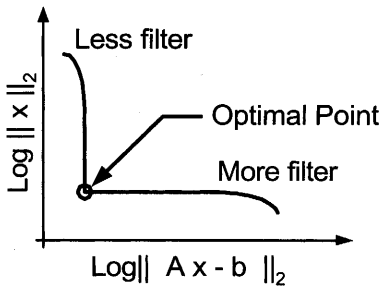

Fig. 2 The L-curve

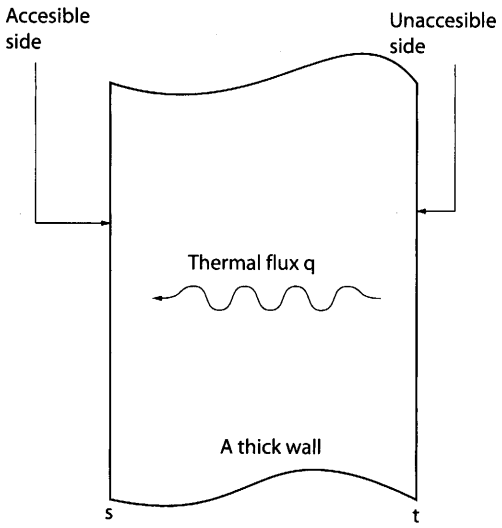

Fig. 3 An example of inverse of heat conduction problem

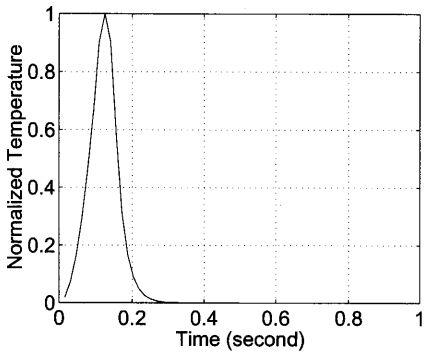

(a) The exact solution $\boldsymbol{x}$

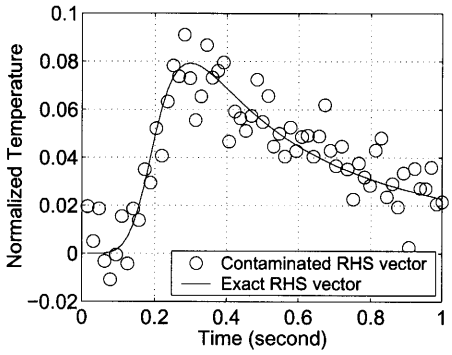

(b) Exact and contaminated RHS vector $\boldsymbol{b}$

Fig. 4 The contaminated right-hand side and exact solution vectors

2.1 Convergence of Conjugate Gradient method

As stated above, the CG method has inherent numerical regularization. This section examines the effect of the regularization to the solution. For simplicity, the analysis was performed using an ill-posed 1-D heat conduction problem as depicted in Fig. 3. The problem having condition number in order of 1.0 E+30. The temperature on the s side is related with the temperature on the t side by a convolution equation with a kernel

$$k(s-t)=\frac{(s-t)^{-3/2}}{2\kappa\sqrt{\pi}}e^{\frac{1}{4\kappa^2(s-t)^2}} \tag{6}$$

where $\kappa=1$.

In this example, the vector $\boldsymbol{x}$ is a temperature-time history at an inaccessible location and also as parameter to be inferred. The right-hand side vector $\boldsymbol{b}$ is a measured temperature-time history at the accessible side. The exact and the noise-contaminated right-hand side vector are plotted in Fig. 4 (b), while the exact solution is plotted in Fig. 4 (a). The noise assumed has Gaussian distribution with a ratio of noise to signal 0.01.

The CG iterative calculation is implemented to compute an optimal solution, and the following convergence criteria are examined:

1. The norm of residual vector $\|\boldsymbol{r}\|_2$,
2. The norm of improvement of the solution vector $\|(\boldsymbol{x}_i-\boldsymbol{x}_{i-1})\|_2$ and
3. The norm of the solution vector $\boldsymbol{x}$.

The iteration initialization is assumed as $\boldsymbol{x}_0=0$. This initialization is similar with the situation having no priori information before hand. Using CG algorithm, the convergent solution is always obtained[7]. The convergence of the CG algorithm to the true solution in the finite number of iterations is achieved in the absence of rounding error[8].

In this section, only a small ill-posed problem is considered to observe the evolution of solution vector $\boldsymbol{x}$ along iteration and evolution of convergence criteria. The results of this study are shown in Figs. 5 to 9. In this case, the best solution is reconstructed after 14 iterations as compared to the exact solution in Fig. 6.

From the results as given Figs. 5 to 9, some properties are observed. As depicted in Fig. 5, begin at the initialization, the solution $\boldsymbol{x}$ approaches the exact solution and then diverge to a noise dominated solution. Figures 7 and 8 shows both $\boldsymbol{r}$ and $\boldsymbol{x}_i-\boldsymbol{x}_{i-1}$ decrease gently until an optimal solution is reached and then both norms oscillates. A curve similar to an L-curve in the Tikhonov-SVD method can be constructed along iteration as depicted in Fig. 9. In the curve, the optimal solution is located in the curve corner as well.

For a summary of this study, the convergence be-

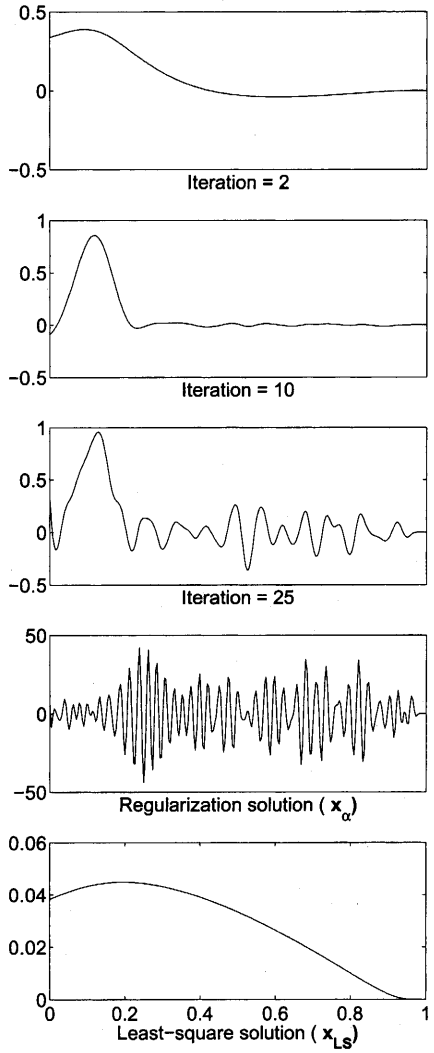

Fig. 5 Estimated temperature as a function of number of iteration (x-axis is the normalized time and y-axis is the normalized temperature)

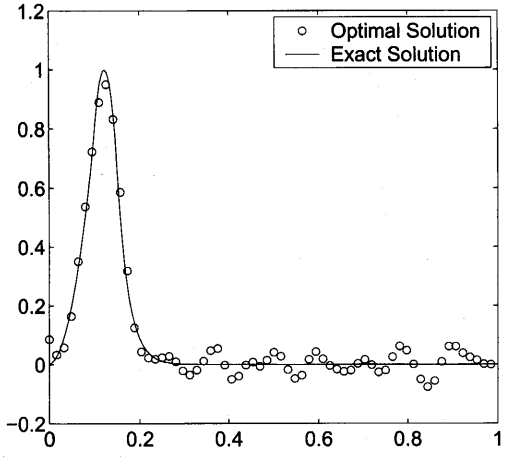

Fig. 6 The optimal estimated temperature $\boldsymbol{x}$

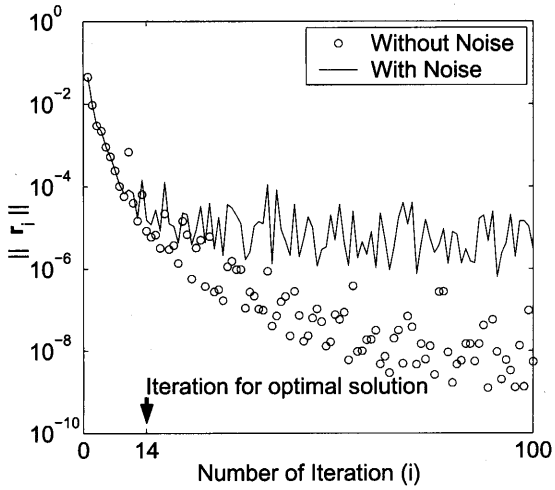

Fig. 7 The residual norms versus number of iteration

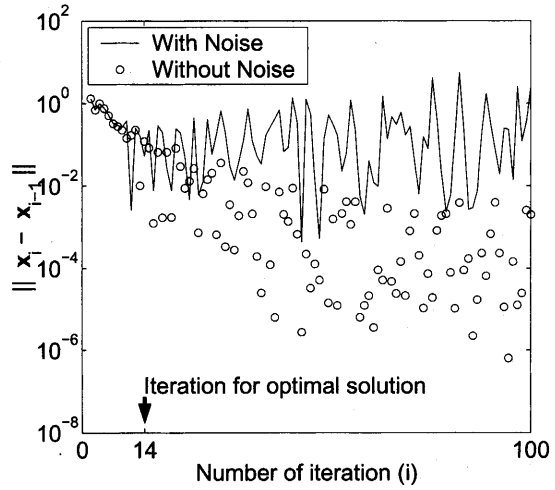

Fig. 8 The residual versus vector norm

havior of CG algorithm is illustrated in the Fig. 10. The iteration begin at the initial vector $\boldsymbol{x}_0$, and then the solution converges very fast to reach the optimal solution $\boldsymbol{x}_{\text{Optimal Solution}}$. If one of the convergence criterion is satisfied, the iteration is finished, otherwise, the iteration will continue and then the solution diverges to the $\boldsymbol{x}_{\text{Reg. Solution}}$.

2.2 Total least-square method

In the total least-square formulation, the system matrix $\boldsymbol{A}$ and the right-hand side vector $\boldsymbol{b}$ are assumed to be contaminated by noise, and then total least-squares solution may be obtained by solving the following equation[11],

$$\begin{pmatrix} \boldsymbol{A}^T\boldsymbol{A} & \boldsymbol{A}^T\boldsymbol{b} \\ \boldsymbol{b}^T\boldsymbol{A} & \boldsymbol{b}^T\boldsymbol{b} \end{pmatrix}\begin{pmatrix} \boldsymbol{x} \\ -1 \end{pmatrix} = \sigma_{n+1}^2 \begin{pmatrix} \boldsymbol{x} \\ -1 \end{pmatrix} \tag{7}$$

where σ_{n+1} is the smallest singular value of augmented matrix [$\boldsymbol{A}$ $\boldsymbol{b}$]. The above equation is for an eigenvalue problem that should be solved for regularization parameter σ and associated eigenvector $\boldsymbol{x}$. There are many methods concerning with solution of an eigenvalue problem such as bisection, Rayleigh quotient iteration, and orthogonal

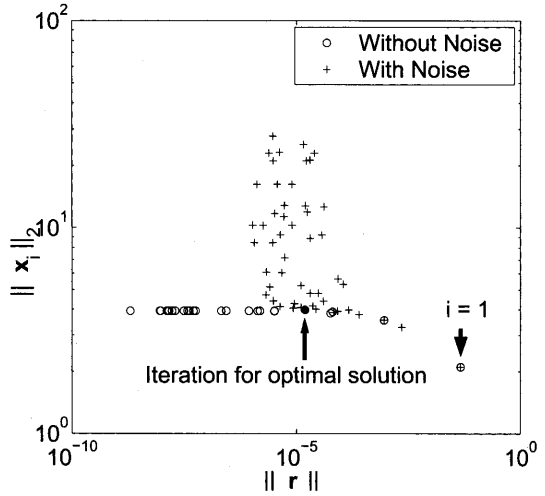

Fig. 9 Residual versus vector norm

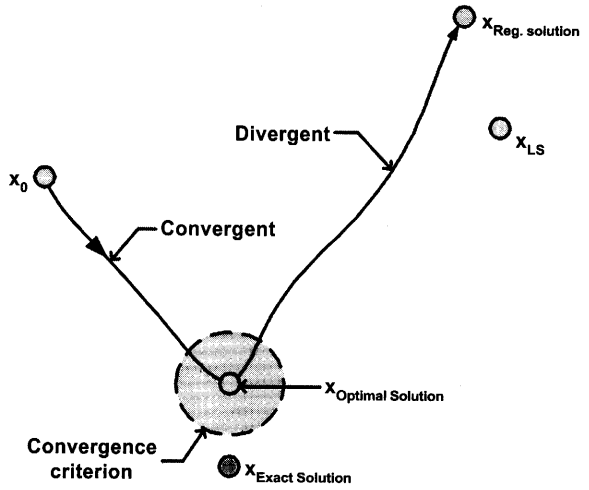

Fig. 10 The convergence properties of CG algorithm

iteration[9]. One approach for solving the TLS problem is proposed by Björck employed the Newton method[11].

In the Björck approach, Eq. (7) is rewritten as a function of σ by following steps. Decompose Eq. (7) into two equivalent form as follow,

$$\boldsymbol{A}^T\boldsymbol{A}\boldsymbol{x}-\boldsymbol{A}^T\boldsymbol{b}=\sigma_{n+1}^2\boldsymbol{x} \tag{8}$$

$$\boldsymbol{b}^T\boldsymbol{A}\boldsymbol{x}-\boldsymbol{b}^T\boldsymbol{b}=-\sigma_{n+1}^2 \tag{9}$$

which can be combined to obtain the following functional equation for σ_{n+1}:

$$\boldsymbol{b}^T\boldsymbol{b}-\boldsymbol{b}^T\boldsymbol{A}(\boldsymbol{A}^T\boldsymbol{A}-\sigma_{n+1}^2)^{-1}\boldsymbol{A}^T\boldsymbol{b}-\sigma_{n+1}^2=0. \tag{10}$$

Therefore, σ_{n+1}^2 is the smallest root of the rational function

$$h(\sigma)=\boldsymbol{b}^T\boldsymbol{b}-\boldsymbol{b}^T\boldsymbol{A}(\boldsymbol{A}^T\boldsymbol{A}-\sigma^2)^{-1}\boldsymbol{A}^T\boldsymbol{b}-\sigma^2, \tag{11}$$

and can be minimized by the Newton method. The Newton algorithm for computing σ and an associated eigenvector can be written as follows:

$k=0$

Initialize $(\sigma^{(-1)})^2$

while $\|(\sigma^{(k)})^2-(\sigma^{(k-1)})^2\|>\epsilon$ do

Solve $(\boldsymbol{A}^T\boldsymbol{A}-(\sigma^{(k)})^2\boldsymbol{I})\boldsymbol{x}=\boldsymbol{A}^T\boldsymbol{b}$ by CG

$(\sigma^{(k+1)})^2=(\sigma^{(k)})^2+\frac{\boldsymbol{b}^T\boldsymbol{b}+\boldsymbol{b}^T\boldsymbol{A}\boldsymbol{x}-(\sigma^{(k)})^2}{1+\boldsymbol{x}^T\boldsymbol{x}}$

$k=k+1$

end while

The above algorithm shows a combination of two iterative methods, i.e., Newton method for searching the regularization parameter σ and the CG for solving a linear system equation. In case where the system matrix $\boldsymbol{A}$ has Toeplitz structure, the FFT method can be employed for matrix-vector multiplication in the CG method. For more than 1000×1000 full matrix $\boldsymbol{A}$, the FFT multiplication is faster than direct multiplication.

3. Numerical Experiments

In this section, the proposed method is applied to some problems in the elasto-dynamic. The first example problem is the estimation of an impulse response function of a single degree of freedom system (SDOF). The second is the estimation of the impact force profile, and the last is identification of viscoelastic material properties. This improvement in the identification method may be extended to more general load profile. It is shown that by applying an inverse analysis method, the deconvolution can be solved safely. The number data in following examples are taken as 2 048 points.

These example problems are having the same governing equation in form of a convolution integral

$$b(t)=\int_0^{\infty}h(t-\tau)x(\tau)d\tau \tag{12}$$

where $h(t)$ is a weighting function or an impulse response function. The function is a complete characterization of the dynamic behavior of a system. In the time domain approach, the deconvolution of Eq. (12) is transformed into an algebra equation form as follow,

$$\boldsymbol{b}=\boldsymbol{A}\boldsymbol{x} \tag{13}$$

where $\boldsymbol{A}$ is a Toeplitz-circulant matrix of $\boldsymbol{h}$ and having size of $n\times n$, $\boldsymbol{b}$ and $\boldsymbol{x}$ are vectors represent the discrete data of $b(t)$ and $x(t)$, respectively. The data are sampled at a fixed interval $T=t_{i+1}-t_i$. The Toeplitz-circulant matrix is a symmetric matrix with respect to it's anti-diagonal line and the matrix is given following,

$$\boldsymbol{A}=\begin{bmatrix} h(t_1) & h(t_N) & \cdots & h(t_3) & h(t_2) \\ h(t_2) & h(t_1) & \cdots & h(t_4) & h(t_3) \\ \vdots & \vdots & \ddots & \vdots & \vdots \\ h(t_{N-1}) & h(t_{N-2}) & \cdots & h(t_1) & h(t_N) \\ h(t_N) & h(t_{N-1}) & \cdots & h(t_2) & h(t_1) \end{bmatrix} \tag{14}$$

For $\boldsymbol{h}$ as the unknown to be sought, Eq. (13) should be rearranged as $\boldsymbol{b}=\boldsymbol{X}\boldsymbol{h}$, where $\boldsymbol{X}$ is a Toeplitz-circulant matrix of $\boldsymbol{x}$.

3.1 Estimation of the impulse response function of a SDOF system

The first example problem is estimation of the impulse response function of a SDOF system. The data of the displacement $\boldsymbol{b}$ and the applied impact force $\boldsymbol{x}$ are necessary for estimation. At beginning, a forward analysis is performed to establish these data. In the analysis, the displacement $\boldsymbol{b}$ is obtain by solving Eq. (13) for given the applied impact force $\boldsymbol{x}$ and the impulse response function $h(t)$. The applied impact force $\boldsymbol{x}$ is taken as a half sine function and the exact impulse response function is computed by

$$h(t) = \frac{1}{m w_d} e^{-\zeta w_n t} \sin(w_d t) \tag{15}$$

where $\omega_n = \sqrt{k/m}$ and $\omega_d = \omega_n \sqrt{1-\zeta^2}$. In this example, the mass m, spring stiffness k and damping ratio ζ are taken as 1.0 kg, 1.0 E+11 N/m, and 0.2, respectively. The total duration of the analysis is taken as 100 μ-second. The condition number of the problem is about 1.0 E+6. The impact forces and their associated responses are show in Fig. 11.

After adding a small noise in the displacement data, an inversion is performed to obtain the impulse response function. The noise level is taken as 1% of the data, and superimposed the data linearly.

The estimated impulse response function using the CG-TLS method is displayed in Fig. 12. In the same figure, the exact solution and the solution given by the TSVD method are presented as well. The figure shows that the method gives an accurate estimation and the solution is slightly better than the TSVD method.

3.2 Impact force estimation

In this section, the total least-square formulation and solution by means of the CG method combined with the Newton method are employed to estimate the impact force. Since the exact solution of the impulse response function of the plate does not exist, a cross checking scheme is used. Figure 13 shows the cross checking scheme which shows that at least load cases are necessary.

One from these two load cases would be the calibration test to obtain the impulse response function. In this paper, the first load case is a triangular form impact force and the second load case is a sine form impact force. The plate is taken as a circular plate and having the thickness of 10 mm and the radius of 100 mm. The impact simulations are performed numerically via the finite element method. The finite element mesh of a 10 degree pie section of the plate is shown in Fig. 14, while the material properties are tabulated in Table 1.

As shown in Fig. 13, the first deconvolution is to establish the impulse response function, and accordingly, the

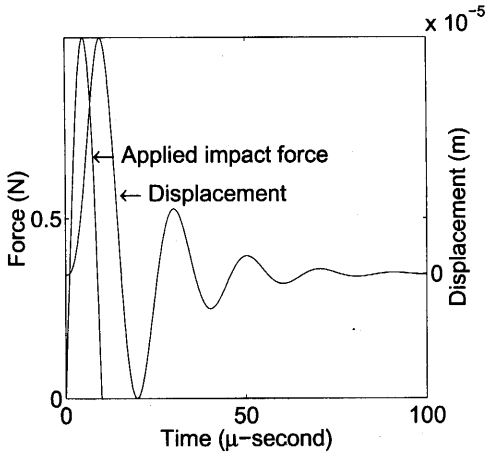

Fig. 11 The applied impact force and associated displacement response

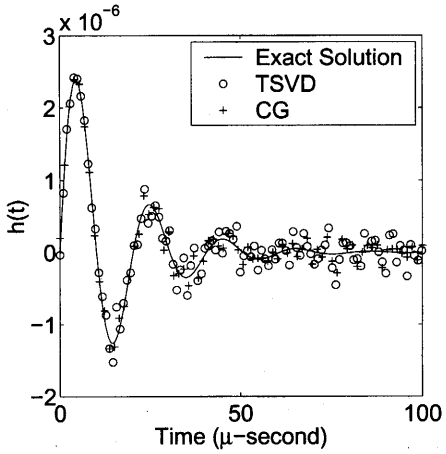

Fig. 12 The estimated impulse response function and comparison with the TSVD method

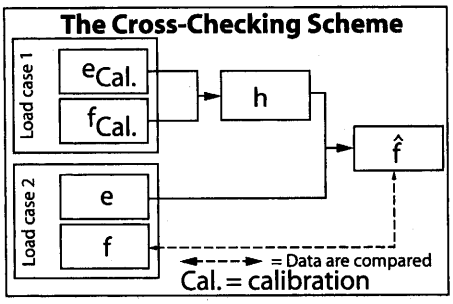

Fig. 13 The cross checking scheme

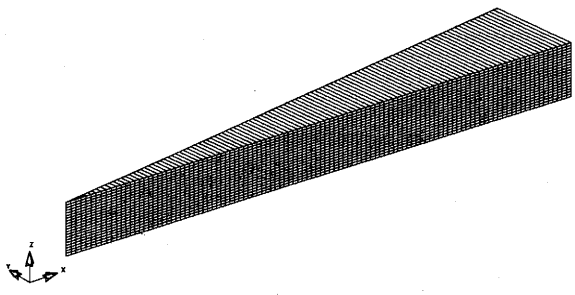

Fig. 14 Finite element mesh

Table 1 Material properties of the plate

Property	Value
Young's modulus	200.0 GPa
Poisson's ratio	0.3
Density	7500.0 kg/m^3

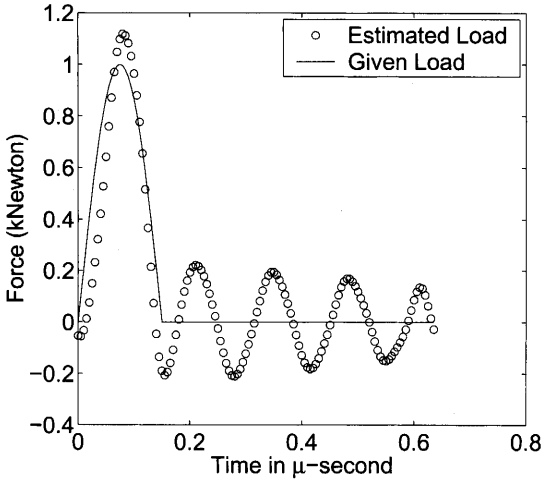

Fig. 15 The sine load function case

second deconvolution is to obtain the estimated impact force. In the first deconvolution, the data set are obtained from the first load set. The result of the impulse response function has condition number in order of 1.0E+16. In the second deconvolution, the estimated impulse response function is deconvolved with respect to the strain time history from the second load set. Figure 15 shows the estimated impact sine force and comparison with the given impact force. The estimated forces in the unloaded region are oscillating around the zero. This behavior in the inverse analysis commonly occurs. The unloaded region contains high frequency components in which the noise exists. The regularization parameter cuts-out the noise and the high frequency parts of the signal as well, and so then the solution vibrates in a low frequency oscillation.

Figure 16 shows the estimated triangular impact force case. In this case, the impulse response function is estimated based on data from the sine case. The result also shows the low frequency oscillation in the flat region.

3.3 Identification of viscoelastic properties of GFRP

Upon application of a load, a viscoelastic material behaves like a combination of an elastic and a viscous material. Such a material may be expressed as Prony-series expansion in an integral form using the kernel function of the generalized Maxwell elements as:

$$G(t)=\sum_{i=1}^{n} G_i e^{-\beta_i t}+G(\infty) \tag{16}$$

where $G(t)$ is current value of material property, n is number of Maxwell elements used to approximate the material relaxation modulus, G_i is give as $C_i(G(0)-G(\infty))$, C_i is

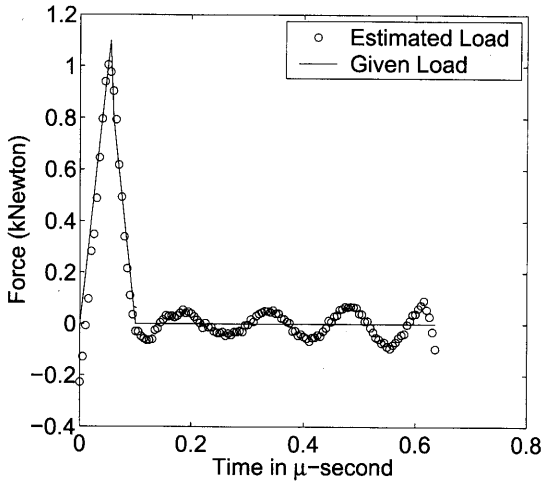

Fig. 16 The estimated triangular impact force

one constants associated with the instantaneous response, $G(0)$ is initial modulus, $G(\infty)$ is final modulus, t is time, and β_i are constants associated with a discrete relaxation spectrum[12].

In this example, for simplicity, it is assumed that the viscoelastic behavior of GFRP may be represented as a single Prony-series. The extension to the several Prony-series is straightforward. The single Prony-series expansion can be written:

$$G(t)=(G(0)-G(\infty))e^{-\beta t}+G(\infty) \tag{17}$$

The GFRP viscoelastic material is also assumed to deform under constant bulk modulus.

Many methods proposed are for identification of viscoelastic material properties, mostly based on the model-fitting-like technique. These methods include the Procedure X method, Collocation method, and Multi-data method[13]. All these methods are only applicable for estimation under a special loading function. It is clear that these special load functions such as impulse function, step function, slope function and harmonic function are difficult to realize in experiments.

This section deals with an inverse analysis method that can be applied for a general type of load profile. The response and the applied stress are related to each other as an convolution equation with an hereditary function or memory function $U(t)$:

$$\epsilon(t)=\int_0^t U(t-u)\sigma(u)du \tag{18}$$

Using Eq. (18) and available data $\epsilon(t)$ and $\sigma(t)$, a stable deconvolution calculation using CG-TLS method can be performed for $U(t)$. By definition, $\epsilon(t)$ is an compliance function if $\sigma(t)$ in Eq. (18) is an unit step function. By knowing $U(t)$ and employing an unit step function for $\sigma(t)$, the above equation can be solved again for an compliance function $J(t)$. The identification of $G(0)$, $G(\infty)$ and β is performed in the following steps:

Table 2 The estimated viscoelastic parameters

No.	Load Profile	$\hat{G}(0)$	$\hat{G}(\infty)$	$\hat{\beta}$
1	Sine function	15.2	6.5	4940
2	Triangle function	14.2	7.5	4800
3	Trapezoid function	13.5	6.9	5010

1. A particular values of viscoelastic properties are assumed for one viscoelastic material, those are $G(0) = 14.1$ GPa, $G(\infty) = 7.1$ GPa, and $\beta = 5000$ 1/sec.

2. A viscoelastic dynamic finite element analysis is performed for given data $\sigma(t)$ and $\epsilon(t)$ is calculated.

3. Solve the deconvolution of Eq. (18) using Newton-CG method for $U(t)$.

4. Convolve $U(t)$ and an unit step stress for compliance function $J(t)$.

5. Applied the least-square curve-fitting to the data $J(t)$ for $G(0)$, $G(\infty)$ and β in Eq. (17).

The estimation was performed under 3 types of load profiles, and then the estimated viscoelastic parameter are shown in Table 2. The estimated viscoelastic parameters shown in the Table 2 are very close to the given parameters. The discrepancy between the estimated initial modulus and the present modulus is less than 8%, and the disrepancy of the final modulues $G(\infty)$ is less than 10%. A good estimation is obtained for relaxation time β where the discrepancy is less than 5.0%.

4. Conclusions

The improved iteration solution developed by this work is very useful for large elasto-dynamic inverse problems. Concerning the developed method, the following conclusions are deduced:

1. In the CG algorithm for solving an ill-posed problem, the convergence criterion plays a very significant role. The L-curve like technique can be used to estimate the optimal number of iterations that satisfies the minimum residual criterion and the minimum norm of $\boldsymbol{x}$ criterion.

2. The total least-square formulation that can be solved by combination of Newton-CG method gives very convenient formulas for solving an ill-posed problem since the regularization parameter and the solution vector can be solved at once.

References

(1) Beck, J.V., Function Specification Method for Solution of the Inverse Heat Conduction Problem, Inverse Problems in Diffusion Process, Proceedings of the GAMM-SIAM Symposium, edited by Engl, H.W. and Rundell, W., (1995), pp.1–18.

(2) Lamm, P.K., Local Regularization Methods for Linear Inverse Problem, Proceedings Sixth Inverse Problem in Engineering Seminar, edited by Murio, D.A., University of Cincinnati, (1994).

(3) Lagendijk, R.L. and Biemond, J., Iterative Identification and Restoration of Images, (1991), Kluwer Academic Publishers, Boston.

(4) Inoue, H., Kishimoto, K., Shibuya, T. and Koizumi, T., Estimation of Impact Force by Inverse Analysis, Inverse Problem in Engineering Mechanics, IUTAM Symposium Tokyo 1992, edited by Tanaka, M. and Bui, H.D., (1993), Springer-Verlag.

(5) Doyle, J.F., Determining the Contact Force during the Transverse Impact of Plate, Experimental Mechanics, Vol.27 (1997), pp.68–72.

(6) Hansen, P.C., Rank-Deficient and Discrete Ill-Posed Problems, (1998), SIAM, Philadelphia.

(7) Sarkar, T.K., Tseng, F.I., Rao, S.M., Dianat, S.A. and Hollmann, B.Z., Deconvolution of Impulse Response Function Time-Limited Input and Output: Theory and Experiment, IEEE Transactions on Instrumentation and Measurement, Vol.IM-34, No.4 (1985), pp.541–546.

(8) Hageman, L.A. and Young, D.M., Applied Iterative Method, (1981), Academic Press, New-York.

(9) Golub, G.H. and Van Loan, C.F., Matrix Computations, (1989), The Johns Hopkins University Press, London.

(10) Huffel, S.V. and Vandewalle, J., The Total Least-Squares Problem: Computational Aspects and Analysis, (1991), SIAM, Philadelphia.

(11) Björck, A., Newton and Rayleight Quotient Methods for Total Least-Squares Problem, edited by Huffel, I.S.V., Recent Advanced in Total Least Squares Techniques and Errors-in-Variable Modeling: Proceedings of the Second International Workshop on Total Least Squares and Errors-in-Variables Modeling, (1997), SIAM, Philadelphia.

(12) Kohnke, P., ed., ANSYS—Theory Reference Manual, (1994), pp.4.46–4.47, ANSYS, Inc., Canonsburg, PA.

(13) Tschoegl, N.W., The Phenomenological Theory of Linear Viscoelastic Behavior—An Introduction, (1989), Springer-Verlag, Berlin.